



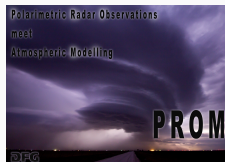
# All Hands Meeting - POLICE

---

Armin Blanke

October 15, 2020

Institute of Geosciences  
Meteorology Section



# First objectives and overall motivation

---

1. Improve our understanding of the origin of  $K_{DP}$ -bands
2. Development of a radar polarimetry algorithm to distinguish between aggregation and riming
3. Evaluation of ice microphysical retrievals with observations

# Olympic Mountains Ground Validation Experiment (OLYMPEX)

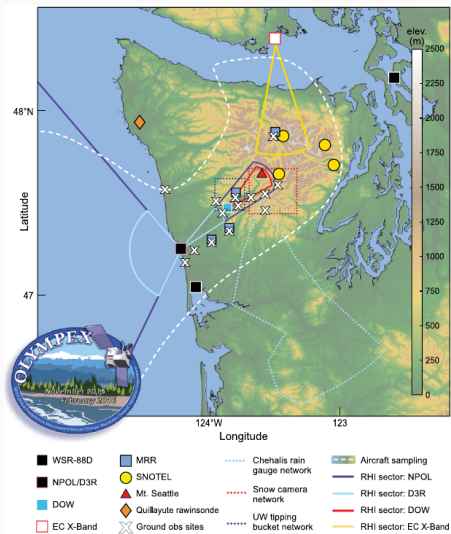


Figure 1: Map of observation network. Radars are shown as squares.

# Doppler on Wheels (DOW)

- Mobile X-band radar
- Frequency: 9.4 GHz (Wavelength:  $\sim 3.2$  cm)
- Range: 59.96 km
- Gate length: 75 m



Figure 2: Mobile X-band radar (Doppler on Wheels).

# Scan strategy (DOW)

RHIs in a 22 degree azimuthal sector over a time period of 3:50 minutes ( $\sim 10$  seconds per azimuth scan)

Elevations: 0 to 71 degrees

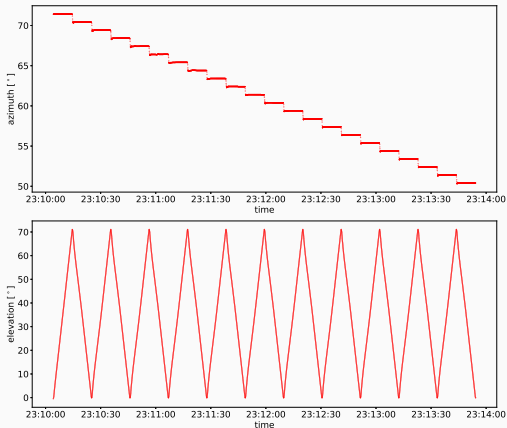


Figure 3: Scan strategy: azimuth and elevation each against time.

# UND Citation aircraft

- Science aircraft University of North Dakota's (UND) Cessna Citation II equipped with an advanced in-situ cloud payload which provides in-situ microphysics

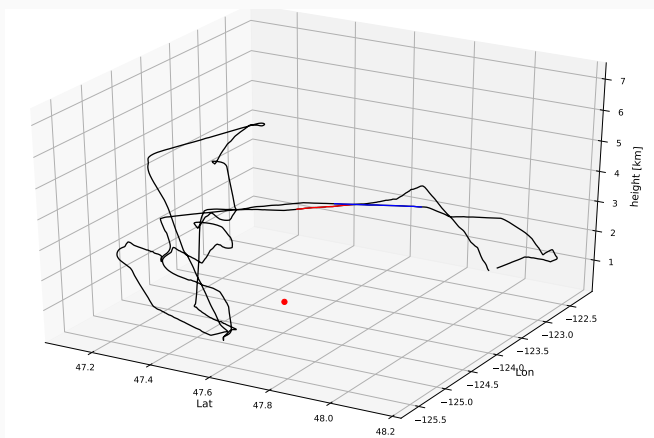
Citation	King Hot Wire Probe	Liquid water, $0.02\text{--}5.0\text{ g m}^{-3}$
	CloudDroplet Probe (CDP)	Cloud droplet size distribution, 2–50 $\mu\text{m}$ range
	2D-S	Particle images, 10 $\mu\text{m}$ –1280 $\mu\text{m}$
	HVPS-3 (2 units)	Particle images, 150 $\mu\text{m}$ –1.92 cm; One horizontal and one vertically-oriented instrument
	CPI	Cloud particle imager; particle imagery at 2.3 m resolution
	CSI	Cloud water content, 0.02 - $\sim 1.0\text{ g m}^{-3}$
	2DC	Particle images, 30–960 $\mu\text{m}$
	Nevzorov	Total water content, 0.02 - $\sim 1.5\text{ g m}^{-3}$
	Rosemount icing probe (RICE)	Supercooled water detection

Table 1: Measuring instruments of the Citation aircraft.

# Citation flight path

21 flight missions in total

Example flight path trajectory:



**Figure 4:** Flight path of the Citation aircraft on 13.12.2015. Location of the DOW red dot. Two flight transects (red and blue) with matched space-time coordinates.

# Co-location DOW und Citation

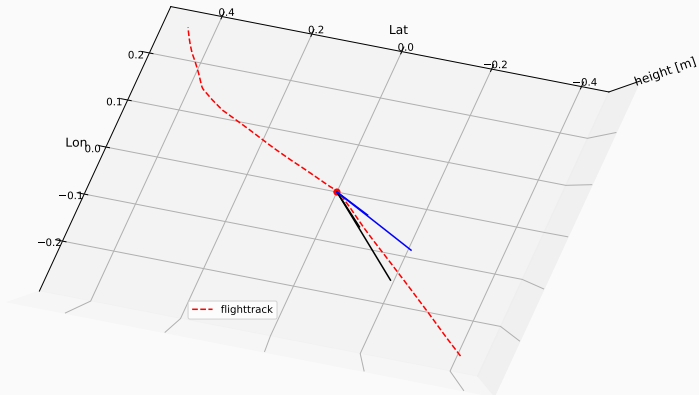


Figure 5: Plan view of one flight transect.



# RHI-QVP (Allabakash et al. 2019)

- Method for displaying and processing RHI scans in a time-height format
- Averaging of polarimetric radar variables from several elevation angles within a certain grid spacing at a fixed azimuth angle

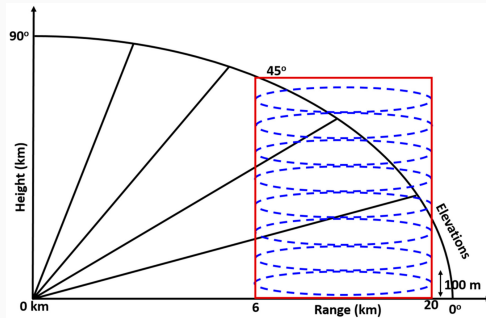


Figure 6: Schematic representation of the R-QVP strategy.

## Adjustments and procedure for creating sector R-QVP

1. Averaging of data within a specified sector in range and azimuth using multiple elevation angles
2. Predefined window at a certain distance with arbitrary length
3. Horizontal averaging via height bins (vertical resolution of 75 m)
4. Extract one vertical column per time span
5. The vertical columns are combined and presented in the sector R-QVP
6. Thresholds:  $\rho_{hv} > 0.7$  and  $60 \text{ dBz} > Z_H > 0 \text{ dBz}$

# Plan view illustration sector R-QVP

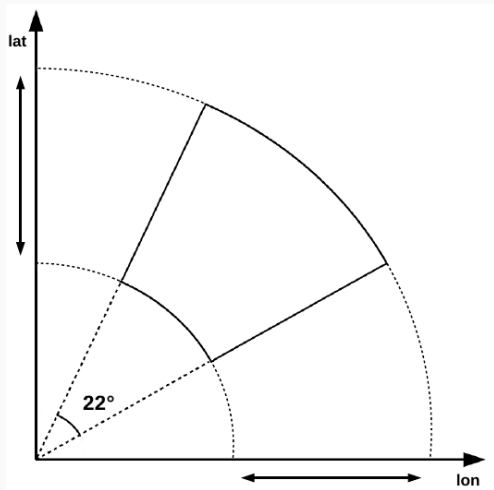


Figure 7: Plan view of a Sector R-QVP.

# Sector R-QVPs: Polarimetric variables

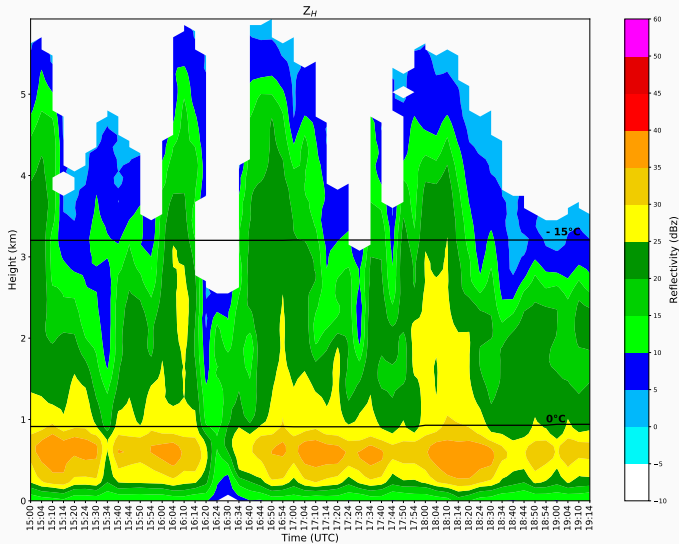


Figure 8: Sector R-QVP of  $Z_H$  on 13.12.2015. The black lines show isotherms of the ERA5 reanalysis at the DOW site.

# Sector R-QVPs: Polarimetric variables

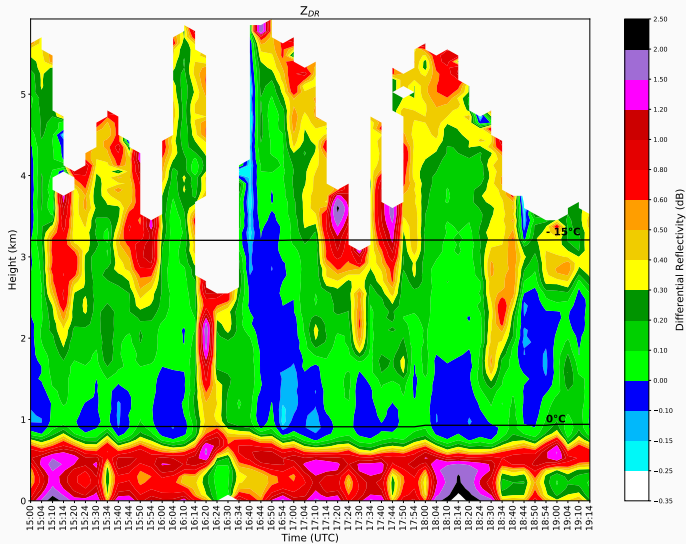


Figure 9: Sector R-QVP of  $Z_{DR}$  on 13.12.2015. The black lines show isotherms of the ERA5 reanalysis at the DOW site.

# Sector R-QVPs: Polarimetric variables

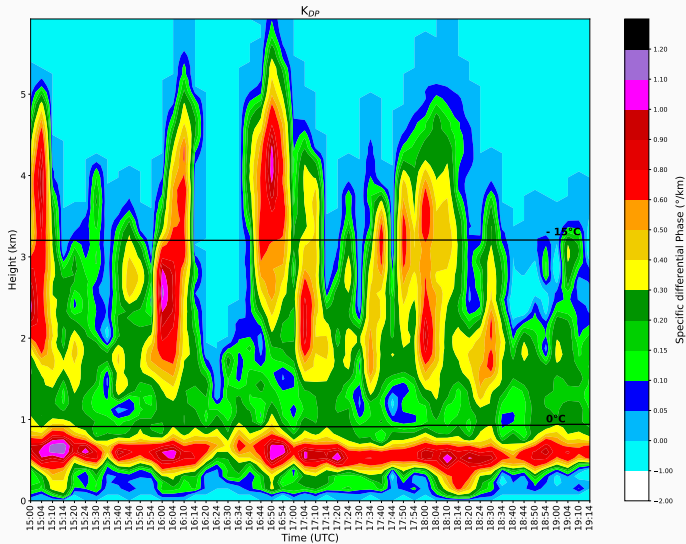


Figure 10: Sector R-QVP of  $K_{DP}$  on 13.12.2015. The black lines show isotherms of the ERA5 reanalysis at the DOW site.

# Cloud Particle Imager images

- first DOW overpass conducted on 13 December 2015 confirmed clear signs of riming
- During the second overpass no evidence of riming is observed

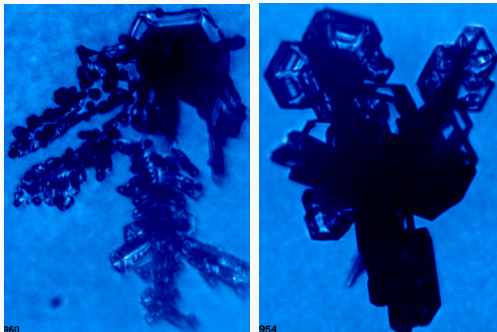


Figure 11: Hydrometeors recorded by the CPI: rimed crystals (16:13 UTC) and unrimed crystals (18:45 UTC).

# Further work

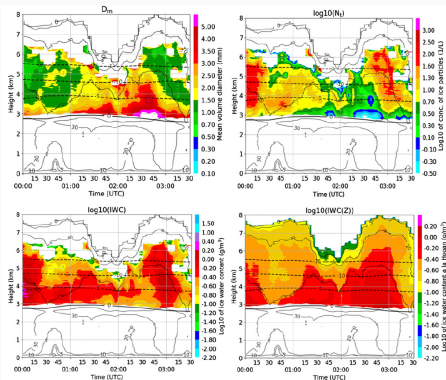


Figure 12: Polarimetric ice microphysical retrieval example (Trömel et al. 2019).

- use state-of-the art polarimetric ice microphysical retrievals for comparison with co-located in-situ measurements (applied to sector R-QVPs)



# Further work

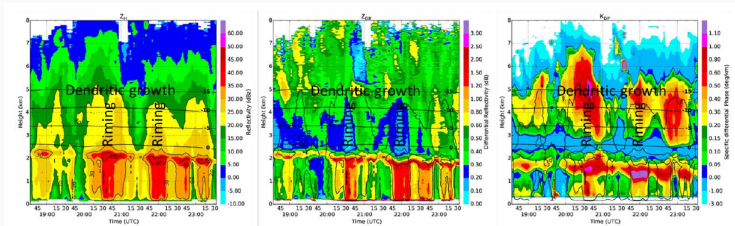






Figure 13: Riming detected in QVPs (Figure adapted from Ryzhkov et al. 2016).

- Detection of polarimetric fingerprints (riming) in R-QVPs
- Development of radar algorithms that distinguish between aggregation and riming with a combination of multiple indicators sided with in-situ observations

## References

---

-  S Allabakash et al. “X-Band Dual-Polarization Radar Observations of Snow Growth Processes of a Severe Winter Storm: Case of 12 December 2013 in South Korea”. In: *Journal of Atmospheric and Oceanic Technology* 36.7 (2019), pp. 1217–1235.
-  Robert A Houze Jr et al. “The olympic mountains experiment (OLYMPEX)”. In: *Bulletin of the American Meteorological Society* 98.10 (2017), pp. 2167–2188.

-  Alexander Ryzhkov et al. “Quasi-vertical profiles—A new way to look at polarimetric radar data”. In: *Journal of Atmospheric and Oceanic Technology* 33.3 (2016), pp. 551–562.
-  Silke Trömel et al. “Polarimetric radar variables in the layers of melting and dendritic growth at X band—implications for a nowcasting strategy in stratiform rain”. In: *Journal of Applied Meteorology and Climatology* 58.11 (2019), pp. 2497–2522.



# All Hands Meeting - POLICE

---

Armin Blanke

October 15, 2020

Institute of Geosciences  
Meteorology Section